Essential Features of the Catalytic Core of Peptidyl-α-hydroxyglycine α-Amidating Lyase†

Aparna S. Kolhekar,‡ Joseph Bell, Eric N. Shiozaki,§ Lixian Jin,|| Henry T. Keutmann,⊥ Tracey A. Hand,|| Richard E. Mains, and Betty A. Eipper*

Department of Neuroscience, University of Connecticut Health Center, Farmington, Connecticut 06030-3401

Received April 25, 2002; Revised Manuscript Received July 29, 2002

ABSTRACT: Bioactive peptides frequently terminate with an essential α-amide that is generated from a COOH-terminal Gly in a two-step enzymatic process occurring within the lumen of the secretory pathway. The first enzyme, peptidylglycine α-hydroxylating monooxygenase, is a member of the copper- and ascorbate-dependent monooxygenase family. The second enzyme, peptidyl-α-hydroxyglycine α-amidating lyase (PAL, EC 4.3.2.5), has no known homologues. Examination of the catalytic core of PAL (PALcc) using trypsin, BNPS skatole, and COOH-terminally truncated proteins failed to identify stable subdomains. Treatment of PALcc with divalent metal ion chelators inactivated the enzyme and increased its protease and thermal sensitivity, suggesting a structural role for bound metal. Purified PALcc contained 0.7 ± 0.4 mol of zinc/mol of enzyme. Since the four Cys residues in PALcc form two disulfide bonds, potential Zn ligands include conserved Asp, Glu, and His residues. The secretion and activity of PALcc bearing mutations in each conserved Asp, Glu, and His residue were evaluated. Mutation of three conserved Asp residues and two conserved His residues yielded a protein that could not be secreted, suggesting that these residues play a structural role. Analysis of mutants that were efficiently secreted identified three His residues along with single Asp residue that may play a role in catalysis. These essential residues occur in a pattern unique to PAL.

The α-amidation of peptides requires the sequential action of two enzymes, peptidylglycine α-hydroxylating monooxygenase (EC 1.14.17.3) (PHM)[1] and peptidyl-α-hydroxyglycine α-amidating lyase (EC 4.3.2.5) (PAL, also peptidylamidoglycolate lyase or PGL) (Figure 1A) (*1*−*6*). In vertebrates, both catalytic domains are expressed as part of a bifunctional precursor protein, peptidylglycine α-amidating monooxygenase (PAM). Like many multifunctional enzymes, the catalytic domains of PAM can function independently. In *Drosophila* and in cnidarians (sea anemone), the two enzymes are encoded by separate genes (*7*−*10*).

PHM is homologous to dopamine β-monooxygenase (EC 1.14.17.1), and the 286-amino acid region of PHM and DBM that is 30% identical is entirely included within the 314-amino acid catalytic core of PHM (*8*−*10*). Prior biochemical characterization of DBM greatly facilitated biochemical and mutational analysis of PHM (*11*−*13*). In contrast, no homologues of PAL have been identified. Enzymes such as ureidoglycolate lyase (EC 4.3.2.3), which catalyze a similar reaction, have not been cloned.

Like PHM, PAL exhibits wide substrate specificity, catalyzing the hydrolytic cleavage of peptidyl-α-hydroxyglycine substrates containing every amino acid at the penultimate position (*14*). The α-hydroxyglycine intermediates produced by PHM and upon which PAL acts are both of the *S* configuration (*4*, *15*) (Figure 1A). Nonpeptide substrates such as α-hydroxyhippuric acid also serve as substrates for PAL (*15*). The pH optimum of PAL is broad, with little change in activity between pH 4.5 and 7.0; the reaction proceeds nonenzymatically as the pH is increased above pH 7 (*15*−*17*). Studies with chelators suggested a role for divalent metals in the reaction catalyzed by PAL (*6*). The soluble, bifunctional amidating enzyme contained copper, as expected, but also contained zinc (*18*). On the basis of its role in other hydrolytic reactions, a zinc-coordinated water or hydroxide could serve as a general base to abstract the hydroxyl proton of the carbinolamide (*18*−*20*) (Figure 1A).

Since PAL plays an essential role in the amidation of peptides, we undertook studies aimed at identifying its catalytic core (PALcc) and defining its essential properties. We demonstrate that PAL lacking any N-linked oligosaccharide is fully active and binds zinc. Disulfide bonds were assigned, with analysis of truncation mutants supporting the folding of PALcc into a single domain. We used sensitivity to thermal denaturation and proteolytic attack to

† Supported by NIH Grant DK-32949.

* To whom correspondence should be addressed: Neuroscience Department, MC-3401, University of Connecticut Health Center, 263 Farmington Ave., Farmington, CT 06030-3401. Phone: (860) 679-8898. Fax: (860) 679-1885. E-mail: eipper@uchc.edu.

‡ Current address: Biopharmaceutical Development Program, SAIC-Frederick, Frederick, MD 21702.

§ Current address: Department of Molecular Biology, Princeton University, Princeton, NJ 08544.

|| Current address: Johns Hopkins University School of Medicine, Baltimore, MD 21205.

⊥ Current address: Endocrine Unit, Massachusetts General Hospital, Boston, MA 02114.

[1] Abbreviations: PHM, peptidylglycine α-hydroxylating monooxygenase; PAL, peptidyl-α-hydroxyglycine α-amidating lyase; PAM, peptidylglycine α-amidating monooxygenase; DBM, dopamine β-monooxygenase.

10.1021/bi0260280 CCC: $22.00
Published on Web 09/19/2002

A. Sequential Reactions Catalyzed by PHM and PAL

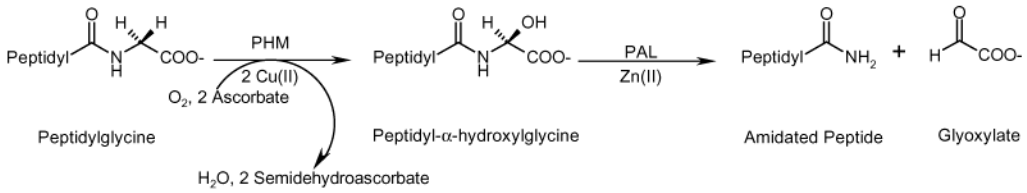

B. Conserved Residues in PALcc

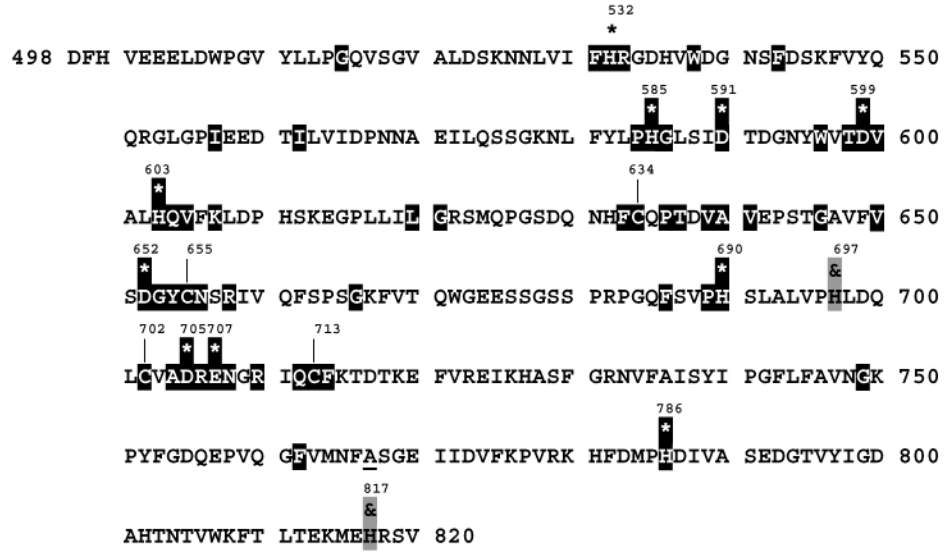

FIGURE 1: Conserved residues in PALcc. (A) The sequential stereospecific reactions catalyzed by PHM and PAL are shown (*15*). (B) The sequences of human (189595), *Drosophila melanogaster* (transcript CT17342; FBgn0020623), *Lymnaea stagnalis* (5353835), *Xenopus laevis* I and II (104156, 113696), and *C. elegans* (AAC16983.1) PAL were aligned with the sequence of rat PALcc (113705) using ClustalW. Except for the *C. elegans* enzyme, each PAL has been expressed and shown to be active. Absolutely conserved residues are shown as white letters on black. Conserved His, Asp, and Glu residues that were mutated are denoted with asterisks above the residue and dark shading; nonconserved His residues mutated as controls are marked with ampersands and gray shading; Cys residues are marked with a vertical bar. Ser[767], part of the N-glycosylation site, was mutated to Ala (indicated by A). The numbering indicates the position in PAM-1 (*43*).

demonstrate a role for metal ions in maintaining the structure of PAL. Site-directed mutagenesis was directed toward conserved Asp, Glu, and His residues (Figure 1B) that might play a role in the binding of zinc to PAL. Residues essential to the successful folding and secretion of PAL and residues essential for catalytic activity were identified.

MATERIALS AND METHODS

Enzyme Assays. The catalytic activity of PAL was assessed using 0.5 μM α-*N*-acetyl-Tyr-Val-α-hydroxyglycine. The substrate was prepared using recombinant PHM (*6*). The enzyme was routinely diluted in 20 mM Na TES (pH 7.4), 10 mM mannitol, 1.0 mg/mL bovine serum albumin, and 1% Triton X-100 (Pierce; Surfact-Amps) and could be frozen and stored without loss of activity. The 40 μL reaction mix routinely contained 5 μL of diluted enzyme, 100−150 mM sodium MES (pH 5.5), and 0.05% Thesit (Boehringer Mannheim). Following incubation for 30 min to 1 h at 37 °C, the substrate and product were separated using ethyl acetate phase separation (*6*). Samples were assayed in duplicate and were diluted to give data in the linear range.

For characterization of divalent metal ion interactions with PALcc, stock salt solutions (32 mM) prepared in water were diluted 8-fold into the reaction mixture. PALcc was assayed following simple addition of each divalent metal or following preincubation with EDTA. The divalent metals were individually assayed for their ability to support nonenzymatic conversion of the substrate to product under standard reaction conditions; no significant amount of product was generated.

Spent medium from hEK-293 cells expressing PALcc was centrifuged to remove debris and concentrated 10-fold using a Centricon with a YM10 membrane (Millipore). Aliquots were diluted to yield a final buffer composition of 75 mM Na MES (pH 5.5), 0.3% bovine serum albumin, and 0.3% Triton X-100 and were incubated at 37 °C for 0−60 min in the presence or absence of 1 mM EDTA. At the end of the 37 °C incubation, aliquots were processed in three separate ways: denatured by boiling into Laemmli sample buffer, diluted into assay diluent with protease inhibitor cocktail and PMSF for assessment of PAL activity, or diluted into 20 mM Tris-HCl (pH 8.0) for trypsin treatment. Trypsin (TPCK; Sigma) (5 mg/mL stock in 1 mM HCl and 5 mM $CaCl_2$) was diluted to 0.25 mg/mL in 20 mM Tris-HCl and used at a final concentration of 0.025 mg/mL.

Purification of PALcc. To prepare large amounts of PALcc, we expressed a chimeric protein in which the signal and pro regions of PAM [rPAM(1−42)] were followed by a His-Met linker and then by rPAM(498−820) with Ser[767] mutated to Ala to eliminate the only N-glycosylation site (Figure 2A) (*8*). Two CHO cell lines (51 and 56) stably

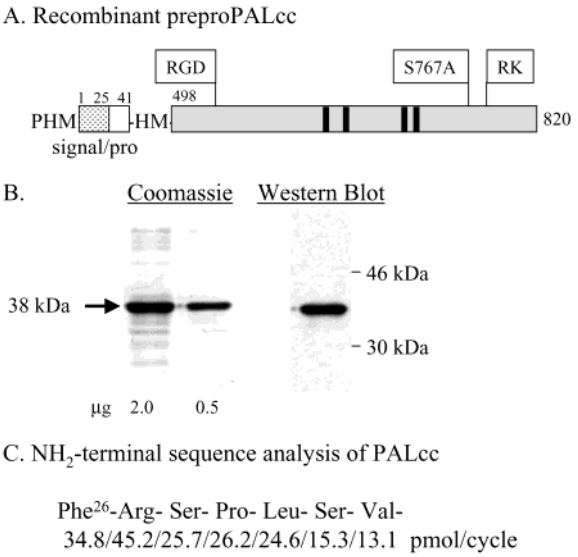

FIGURE 2: Purification of PALcc. (A) The structure of recombinant preproPALcc is shown; the 25-amino acid signal and 16-amino acid pro region of PAM are separated from PAL by a His-Met (HM) linker. The locations of the Arg-Gly-Asp (RGD) putative integrin binding site, the mutated N-glycosylation site [Ser^{767}Ala (S767A)], and the single pair of basic amino acids [Arg-Lys (RK)] are indicated. The four cysteine residues are denoted with thick vertical bars. (B) Purified PALcc fractionated by SDS−PAGE was transferred to an Immobilon membrane and visualized with Coomassie brilliant blue or rabbit polyclonal antibody to rPAM-1(564−582). (C) Purified PALcc was subjected to Edman degradation; the yield of the major amino acid observed at each cycle is indicated. The observed sequence is that expected for the pro segment of PAM, which preceded the sequence of PALcc and is not shown in Figure 1.

transfected with a pCIS vector encoding PALcc were used; methotrexate treatment failed to increase expression levels. In the process of carrying out site-directed mutagenesis of PALcc, we noted a single-nucleotide change introduced into PALcc by a PCR-generated error: nucleotide A^{1949} became G^{1949}; as a result of this mutation, amino acid Gln^{551} was mutated to Arg^{551}, yielding PALcc-QR. PALcc-QR was purified from the spent medium of stably transfected CHO cells grown in roller bottles. Secreted proteins were concentrated by precipitation with $(NH_4)_2SO_4$ (0.442 or 0.611 g/mL); the pellets were resuspended in 20 mM Na TES and 0.5 M $(NH_4)_2SO_4$ (pH 7.4) and applied to a Sephadex G75-120 column (2 cm × 90 cm) equilibrated and eluted with the same buffer. Fractions containing PALcc were identified after SDS−PAGE, pooled, and concentrated 5−10-fold using an Amicon stirred flow cell. The sample was applied to a hydrophobic interaction column (phenyl Superose HR10/10; Amersham Pharmacia Biotech) equilibrated with 20 mM Na TES and 0.5 M $(NH_4)_2SO_4$ (pH 7.4). PALcc was eluted by application of 20 mM Na TES (pH 7.4). PALcc-containing fractions were pooled, and the buffer was adjusted to 20 mM Tris-HCl (pH 8.0) using an Amicon stirred flow cell. Following application to a MonoQ column (HR5/5; Amersham Pharmacia Biotech), PALcc was eluted with a gradient to 20 mM Tris-HCl and 1.0 M NaCl (pH 8.0).

Wild-type PALcc was subsequently expressed in pEAK Rapid hEK-293 cells using the pEAK10 vector (Edge Biosystems). The secretions of transiently transfected PALcc and PALcc-QR were indistinguishable. Stably transfected nonclonal cells expressing PALcc were generated by puromycin selection (0.5 μg/mL for 1 week followed by 1 μg/mL) and grown to confluence in flasks. Cells were then fed daily with CSFM, and protein in the spent medium was concentrated using a Centricon or precipitated using 80% $(NH_4)_2SO_4$. The Q551R mutation had no discernible effect on the K_m or V_{max} of PAL. The sensitivities of PALcc and PALcc-QR to temperature or EDTA were indistinguishable. PALcc-QR was more sensitive to trypsin digestion that PALcc, although both proteins yielded a major 33 kDa product. Two of the site-directed mutants (H532A and H585A) were studied in both wild-type PALcc and PALcc-QR; no differences in secretion rate or catalytic activity were associated with the Q551R mutation. The H817A and D599N mutations were studied in only wild-type PALcc.

Characterization of Purified PALcc. The extinction coefficient (A_{280}) of a 1.0 mg/mL solution of purified PALcc-QR in 20 mM Tris-HCl and 100 mM NaCl (pH 8.0) was 1.42 as determined by quantitative amino acid analysis. Purified PALcc was subjected to Edman degradation in an effort to identify its NH_2 terminus. The K_m for α-*N*-acetyl-Tyr-Val-α-hydroxyglycine was determined by varying the concentration of substrate from 10 to 200 μM. The ability of varying amounts of TPCK-trypsin to attack PALcc or PALcc-QR was evaluated. Following digestion, reactions were stopped by addition of protease inhibitors or by boiling into Laemmli sample buffer. Samples were then assayed for catalytic activity or fractionated by SDS−PAGE. Following transfer to Immobilon, products were visualized with antibody specific for rPAM-1(564−582). For Edman degradation, purified PALcc-QR (1.68 μg) was digested with 0.25 μg of TPCK-trypsin in a final volume of 30 μL of 20 mM Tris-HCl (pH 8.0) for 30 min at 37 °C; the digests were fractionated by SDS−PAGE and transferred to Immobilon membranes, and the products were visualized by staining with Coomassie Brilliant Blue. The 33 kDa product that was obtained was subjected to Edman degradation following transfer to an Immobilon PVDF membrane using an Applied Biosystems model 477A pulsed-liquid sequencer with on-line HPLC identification.

The presence of free sulfhydryl groups in PALcc was evaluated using 5,5′-dithiobis(2-nitrobenzoic acid); both native protein and protein denatured by incubation in 6 M guanidine HCl were analyzed (*21*). For evaluation of disulfide bonds, PALcc-QR purified by RP-HPLC on a μBondapak C4 column was dried by vacuum centrifugation, resuspended in 100 μL of 50% acetic acid, and allowed to incubate with 5 mg of BNPS skatole in the dark, under a nitrogen atmosphere at 37 °C for 48 h (*22*). The sample was centrifuged, and the pellet was suspended in 50 μL of water and centrifuged again; the two supernatants were pooled and extracted three times with 400 μL of ether to remove excess reagent. The aqueous fraction was dried by vacuum centrifugation and dissolved in a 99.9% acetonitrile/0.1% trifluoroacetic acid mixture. Aliquots were removed for analysis by reducing or nonreducing SDS−PAGE. A small aliquot was subjected to Western blot analysis using affinity-purified Ab69 [rPAM-1(564−582)]; the remainder of the sample was subjected to Edman degradation after being transferred to Immobilon PVDF membranes.

Measurement of the Amount of Bound Zn Using 4-(2-Pyridylazo)resorcinol (PAR). Zn(II) bound to PALcc was quantified using a modification of the protocol of Hunt et

al. (*23*). Dilutions of PALcc and reagent were made with 500 mM Hepes/NaOH (pH 7.5); MilliQ water was used throughout. Zn(II) standards (0−30 μM) were prepared by dilution of a 10 mM Zn(II) atomic absorption standard. Enzyme samples were washed with 500 mM Hepes/NaOH (pH 7.5) in a Millipore 30 kDa cutoff microconcentrator. The concentration of PALcc was determined by measuring A_{280}. PALcc was pretreated with 4 mM 2-mercaptoethanol for 5 min at 100 °C before denaturation with 4 M guanidine HCl or 3% perchloric acid at room temperature for 5 min. PAR was freshly prepared in 500 mM Hepes/NaOH (pH 7.5), and 25 μL of denatured protein was added to 125 μL of 100 μM PAR before the absorbance at 500 nm was measured. The Zn(II) content of the denatured enzyme was determined from the standard curve; inclusion of 0.8 mM 2-mercaptoethanol and 0.8 M guanidinium HCl or 0.6% (v/v) perchloric acid in the Zn(II) standard did not alter the measured absorbance.

Site-Directed Mutagenesis and Transient Expression. Conserved His, Asp, and Glu residues (Figure 1B) were individually mutated to Ala, Asn, and Gln, respectively. Complementary mutagenic oligonucleotides were typically 32−36-mers and were inserted into pBS.PALccS767A using the QuickChange site-directed mutagenesis kit (Stratagene). The coding region was sequenced in its entirety, and the presence of the desired mutation was verified. Plasmids with the desired mutation were digested with *Not*I and *Hin*dIII, and the fragment encoding the mutant PALcc was inserted into a mammalian expression vector, pEAK10, prepared with *Not*I and *Hin*dIII (Edge Biosystems, Gaithersburg, MD).

pEAK Rapid hEK-293 cells (Edge Biosystems) were plated in 30 mm dishes, allowed to grow for 1 day, and transfected with 15 μg of plasmid DNA using lipofectamine (GIBCO BRL, Rockville, MD). Cells were fed 10 h later with fresh growth medium; 24 h after application of the DNA, cells were rinsed with CSFM for 1 h. Fresh CSFM (3.0 mL) was then applied, and spent medium was collected 24 h later; PMSF and protease inhibitor mix were added after centrifugation (*24*). Cells were harvested into 0.5 mL of 20 mM sodium TES, 10 mM mannitol, and 1% Triton X-100 (pH 7.0) containing protease inhibitors and frozen. Before analysis, cell extracts were centrifuged (14000*g* for 5 min) to remove insoluble material, and the protein content was determined using the BCA assay (Pierce Chemical Co.) with bovine serum albumin as a standard.

Aliquots of cell extract and medium were assayed for catalytic activity and analyzed by Western blot. Where indicated, assays were carried out on spent medium that had been concentrated 6−15-fold using a Centricon with a YM10 membrane (Millipore). Mutants that failed to yield detectable amounts of secreted PALcc on an overexposed Western blot and failed to yield activity that was above the level observed in nontransfected hEK-293 cells were categorized as malfolded and were not further characterized. For PALcc mutants yielding secreted protein, enzyme activity in the Centricon-concentrated samples of medium was quantified so that equal amounts of enzyme activity could be subjected to Western blot analysis. Kinetic parameters (K_m and V_{max}) were determined by varying the concentration of Ac-Tyr-Val-hydroxyglycine from 1 to 120 μM. At least two independent transfections were analyzed for each mutant.

The stability of the malfolded PALcc mutants was determined by carrying out pulse−chase metabolic labeling experiments on transiently transfected pEAK Rapid cells. Cells transiently expressing PALcc were analyzed simultaneously for comparison. Replicate 10 mm wells of transiently transfected pEAK Rapid cells were incubated in medium containing [^{35}S]Met for 15 min and either harvested immediately (pulse) or further incubated for variable amounts of time in medium lacking radiolabeled Met (chase) (*25*). Cell extracts (pulse and chase) and medium (chase) were immunoprecipitated with antisera to PAL (Ab471 or Ab877), fractionated by SDS−PAGE, and visualized by fluorography.

RESULTS

Purification of PALcc. Expression of active PHM and PAL in bacterial or insect systems has not yet been accomplished, and stably transfected CHO cells have been used to produce both enzymes (*8*, *14*, *26*). To ensure the efficient secretion of monofunctional PAL, we retained both the signal and pro region of PAM (Figure 2) (*25*). The COOH terminus of PALcc was Val^{820}, the residue immediately preceding the Lys^{821}Lys site thought to undergo endoproteolytic cleavage when active PAL is released from integral membrane forms of PAM (*6*, *8*, *9*, *15*, *25*). Following concentration by ammonium sulfate precipitation, PALcc was purified from spent medium by sequential gel filtration, hydrophobic, and ion exchange chromatography. The 38 ± 1 kDa protein (predicted molecular weight of 38 306) was visualized by rabbit polyclonal antisera to bacterially expressed PAL (Figure 2B) as well as antipeptide antisera. Edman degradation indicated that signal peptide cleavage occurred at the expected site after Ala^{25}; the pro region remained attached to the NH_2 terminus of PALcc secreted by CHO cells (Figure 2C).

Optimal PAL activity was observed from pH 5 to 6.5, and the kinetic parameters of purified PALcc were determined at pH 5.5 (Figure 3). Similar K_m values for a peptidyl-α-hydroxyglycine substrate were determined when PALcc was assayed in spent medium without any purification (Figure 3B). Western blot analysis of equal amounts of PAL activity from spent medium or pure PAL revealed equal amounts of PAL protein (data not shown). Purified rat PAM-3 and purified bovine PAL yielded K_m values of 37 ± 15 and 38 ± 13 μM, respectively, in good agreement with the value determined for purified rat PALcc (33 ± 6 μM). The turnover number of purified PALcc was 380 ± 40 s^{-1}, in good agreement with the turnover number of purified bovine PAL (220 s^{-1}) (*1*).

Properties of PALcc. PAL functions in the lumen of the secretory pathway and is secreted upon exocytosis. We used general denaturants, a reductant, and chelators to probe its stability (Figure 4). PAL is quite resistant to general protein denaturants; addition of 0.5 M guanidinium HCl reduced activity to 28% of control, while addition of 1 M urea reduced activity to 58% of control (data not shown). Dose−response curves for the effect of 2-mercaptoethanol, EDTA, EGTA, and *o*-phenanthroline on PAL activity are shown in Figure 4A. PALcc is resistant to reduction by 2-mercaptoethanol, with half-maximal inhibition by 125 mM 2-mercaptoethanol. Both EDTA and EGTA produced 50% inhi-

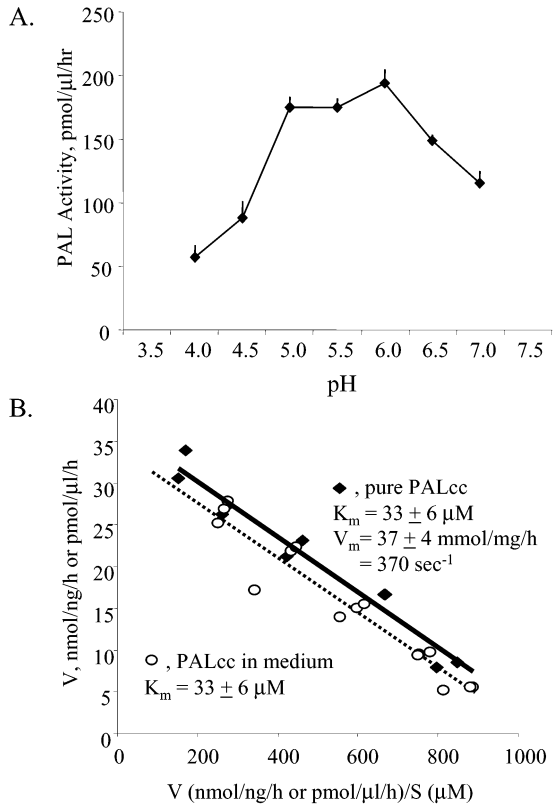

FIGURE 3: Kinetic parameters of PALcc. (A) PALcc in spent medium was diluted and assayed at the indicated pH. (B) The purified enzyme and spent medium from cells expressing PALcc were assayed in the presence of variable amounts of peptidyl-α-hydroxyglycine substrate. The K_m values calculated from the Eadie−Hofstee plots are given. Velocities for purified PALcc are in units of nanomoles per nanogram per hour, while velocities for spent medium are in units of picomoles per microliter per hour.

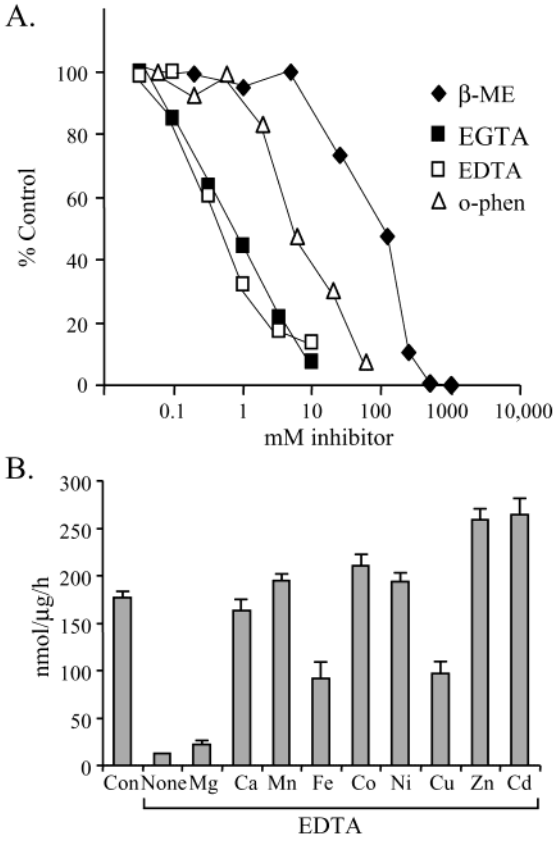

FIGURE 4: Properties of PALcc. (A) An aliquot of purified PALcc was preincubated with the indicated concentration of 2-mercaptoethanol, *o*-phenanthroline, EDTA, or EGTA and then diluted and assayed for activity. Data are normalized to the untreated enzyme assayed at the same time (100%). (B) PALcc was inactivated by incubation with 2 mM EDTA on ice for 10 min; the ability of different divalent cations (4 mM) to restore PAL activity was determined following incubation for an additional 10 min on ice. Error bars show the range of duplicate samples. The experiment was repeated three times with similar results.

bition of PAL when present at a concentration of 0.5−1 mM, while 10-fold more *o*-phenanthroline was required to produce 50% inhibition.

The ability of various metals to restore PAL activity following inhibition by EDTA was evaluated (Figure 4B). Enzyme activity was reduced to <10% of control levels following incubation on ice with 2 mM EDTA. Addition of Zn^{2+} or Cd^{2+} yielded an amount of activity that exceeded control levels by approximately 50%, while addition of Ca^{2+}, Mn^{2+}, Co^{2+}, or Ni^{2+} restored activity to control levels. Full activity was not restored by addition of Mg^{2+}, Fe^{2+}, or Cu^{2+}. Unlike the situation with PHM, restoration of PAL activity was achieved with a variety of divalent metal ions.

Protease Sensitivity of PALcc. We employed trypsin to explore the structure of PALcc (Figure 5). Exposure of PALcc to increasing amounts of trypsin generated a series of intermediates leading to major cleavage products of 33 and 35 kDa (Figure 5A). The rabbit polyclonal antiserum that was used recognizes rPAM(564−582). Removal of the pro region (residues 27−41) (Figure 2A) would be expected to decrease the mass by 2 kDa without reducing catalytic activity. Consistent with this, the products generated by treatment with 5 μg of trypsin are essentially fully active (Figure 5B). In contrast, the catalytic activity of PALcc was largely eliminated following treatment with 50 μg of trypsin, when only the 33 and 35 kDa proteins were present. No smaller stable intermediates were detected, and more extensive digestion failed to yield fragments that could be visualized with this antibody (data not shown).

PALcc bearing a fortuitous Q551R mutation was much more sensitive to digestion by trypsin; a 33 kDa product was generated, but products of intermediate mass were not observed (Figure 5C). Edman degradation of this 33 kDa fragment yielded a sequence that began with Gly^{553}, identifying Arg^{552} as the major site of tryptic cleavage (Figure 5C). Removal of the pro sequence along with rPAM(498−552) would reduce the mass of PALcc by 8.6 kDa, generating a 30 kDa product, close to the mass of the observed product. Our data suggest that trypsin cleavage under these conditions is limited to the NH_2-terminal end of PALcc and was facilitated by the accidental generation of an Arg^{551}-Arg^{552} paired basic cleavage site.

Disulfides. Cysteine residues in secreted proteins are generally present in disulfide bonds (*27*). PALcc contains only four Cys residues, all of which are totally conserved (Figures 1 and 6). Incubation of purified PALcc that had been denatured by incubation in 6 M guanidine HCl with Ellman's reagent [5,5′-dithiobis(2-nitrobenzoic acid)] led to detection of only 0.3 mol of free sulfhydryl/mol of enzyme, suggesting that the four Cys residues form two disulfide bonds. Since disulfide bonds are a major factor determining enzyme structure, we explored their connectivity (Figure 6A).

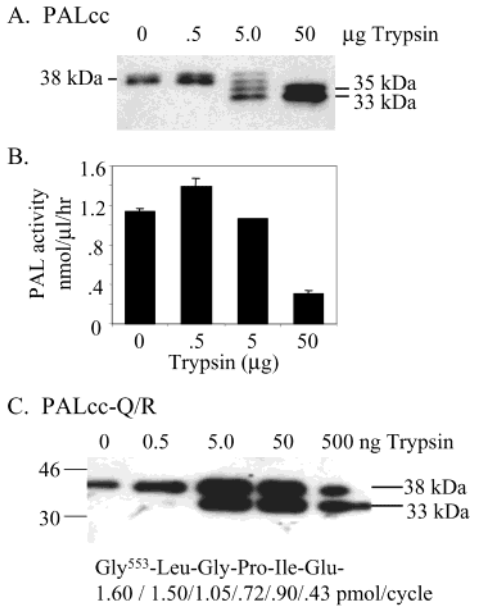

FIGURE 5: Protease resistant fragment of PALcc. An aliquot of spent medium from stably transfected, nonclonal pEAK Rapid hEK-293 cells was diluted into 20 mM Tris-HCl (pH 8.0) and digested for 30 min at 37 °C with the indicated amount of trypsin in a final volume of 30 μL. Digestion was stopped by boiling aliquots in Laemmli sample buffer (A) or by diluting aliquots into assay diluent containing PMSF and protease inhibitor cocktail (B). Products were identified using PAL Ab256; the apparent molecular masses are indicated. (C) Purified PALcc-QR [168 ng in 10 μL of 10 mM Tris-HCl (pH 8.0)] was digested with the indicated amount of TPCK-trypsin at 37 °C for 30 min; aliquots were analyzed by Western blot using PAL Ab471. A separate sample was prepared for Edman degradation. The 33 kDa product, which migrates at the same position as the product obtained from PALcc, yielded a single major sequence shown with picomole yields below the gel. A minor sequence, commencing one residue earlier at Arg^{552}, was also observed due to low-level cleavage at the Q551R mutation.

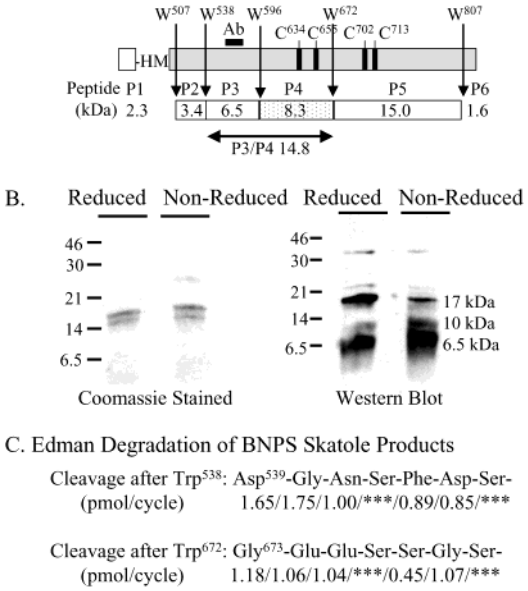

FIGURE 6: Assignment of disulfides in PALcc. (A) Diagram of PALcc showing the location of Cys and Trp residues and the mass for each predicted BNPS skatole peptide (P1−P6). (B) The BNPS skatole-treated protein was analyzed by SDS−PAGE in the absence (nonreduced) or presence (reduced) of 2-mercaptoethanol. Proteins were visualized with Coomassie staining or by Western blot analysis using rabbit polyclonal antisera to rPAM-1(564−582) (Ab69). (C) Edman degradation of the 14−18 kDa BNPS skatole products from a nonreducing gel. Where a Ser occurs in both sequences, relative yields cannot be estimated and data are represented with three asterisks.

There are five Trp residues in PALcc, one of which (W^{672}) occurs between the second and third Cys residues. We therefore used BNPS skatole, a means of chemically cleaving after Trp residues, to investigate the pattern of disulfide bonds (*22*). Two Cys residues reside in peptide P4 (8.3 kDa) and two in peptide P5 (15.0 kDa) (Figure 6). Aliquots of the BNPS skatole digest were fractionated on reducing and nonreducing gels and visualized with Coomassie or with an antiserum to rPAM(564−582), an epitope contained within peptide P3 (6.5 kDa).

If disulfide bonds linked Cys^{634} or Cys^{655} to Cys^{702} or Cys^{713}, a major 23.3 kDa product would be observed on nonreducing gels (P4 with P5). In comparing the Coomassie and Western blot patterns for reducing and nonreducing gels, we observed very similar patterns (Figure 6B). As predicted, a 6.5 kDa peptide was recognized by the antipeptide antibody. However, cleavage by BNPS skatole did not proceed to completion, and larger immunoreactive peptides were also detected, suggesting that P2−P3 and P3−P4 peptides sometimes remained attached. Consistent with this observation, Edman degradation of the 17 kDa, nonreduced product yielded similar amounts of product representing cleavage after Trp^{538} and after Trp^{672} (Figure 6C). P3−P4 and P5 peptides, which cannot be linked by a disulfide bond, comigrated during SDS−PAGE due to their comparable masses (14.8 and 15.0 kDa, respectively). Since disulfide bonds linking residues from P4 to P5 would yield products on nonreducing gels of at least 23.3 kDa, we can conclude that disulfide bridges are formed by neighboring Cys residues (Cys^{634}−Cys^{655} and Cys^{702}−Cys^{713}).

Contribution of Individual Exons to the Structural Domains of PAL. Rat PALcc is encoded by eight exons (exons 17−24) (Figure 7A) (*9*, *28*). Thinking that individual exons might encode functional domains, we appended PAL exons to the entire PHM domain and evaluated the ability of the proteins to acquire a conformation that would allow them to exit the endoplasmic reticulum and be secreted. These five truncated PHM/PAL proteins are identified by their COOH terminus (*9*). Whether secreted or not, each protein yielded active PHM, which served as a positive control. We knew from our earlier investigations that production of active PAL would require all eight exons. While PHM/PAL820s is secreted and active, PHM/PAL778s is not secreted and lacks activity (Figure 7B) (*9*). PHM/PAL741s and PHM/PAL674s are detected in cell extracts but not in medium. In striking contrast, PHM/PAL604s (which has no PAL-derived Cys residues) is efficiently secreted. The lack of secretion of PHM/PAL778s, -741s, and -674s suggests that the presence of a malfolded truncated PAL domain prevents secretion.

To evaluate this possibility, metabolic labeling studies were carried out. For reference, newly synthesized PAM-3 is fully recovered after a 2 h chase and is equally distributed between cells and medium (Figure 7C). Similarly, slightly more than half of the newly synthesized PHM/PAL604s is recovered from cell extracts after a 2 h chase, with the remainder recovered from the medium (Figure 7C). PHM/PAL674s

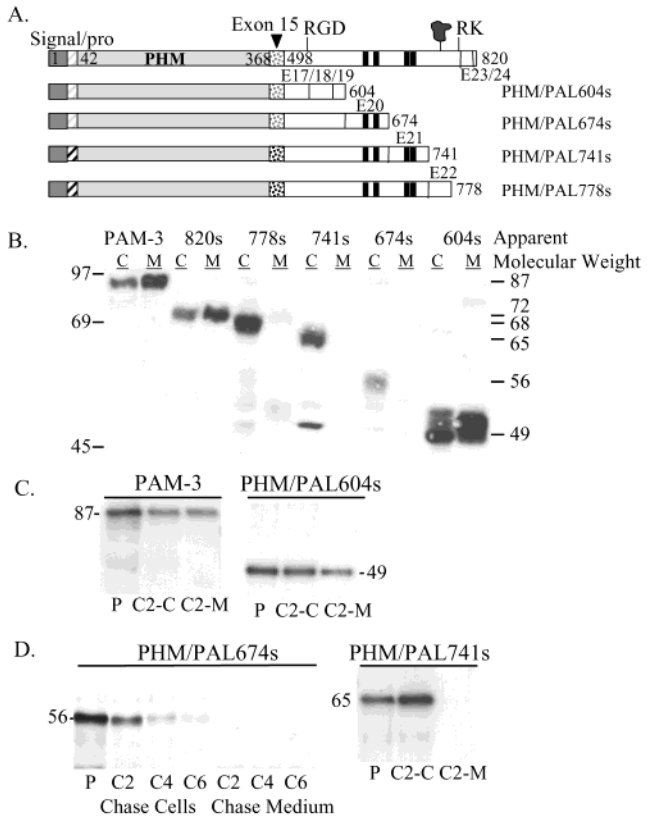

FIGURE 7: Search for folded domains within PALcc. (A) The structures of the expressed PHM/PALs proteins are shown. Each consists of a functional PHM domain [rPAM-1(42−368)] preceded by its normal signal and pro region; exon 15, the flexible hinge region that follows the catalytic core of PHM, is denoted. The PAL exons included in each construct are indicated (E17, etc). Cysteine residues are marked by thick vertical lines, and the N-linked oligosaccharide is indicated by the irregular shape. (B) Aliquots of CHO cell extracts containing 200 pmol/h of PHM activity, and the corresponding volume of medium were subjected to Western blot analysis using an antibody raised to recombinant PAL(498−604) (Ab877). (C and D) Replicate wells of hEK-293 cells expressing the indicated proteins were incubated with [^{35}S]Met/Cys for 15 min and harvested immediately (P) or chased in unlabeled medium for the indicated amounts of time before cells were harvested [chase, cells (C-C)] and medium [chase, medium (C-M)]. Equivalent amounts of cell extract and medium were denatured and immunoprecipitated with the same PAL antibody.

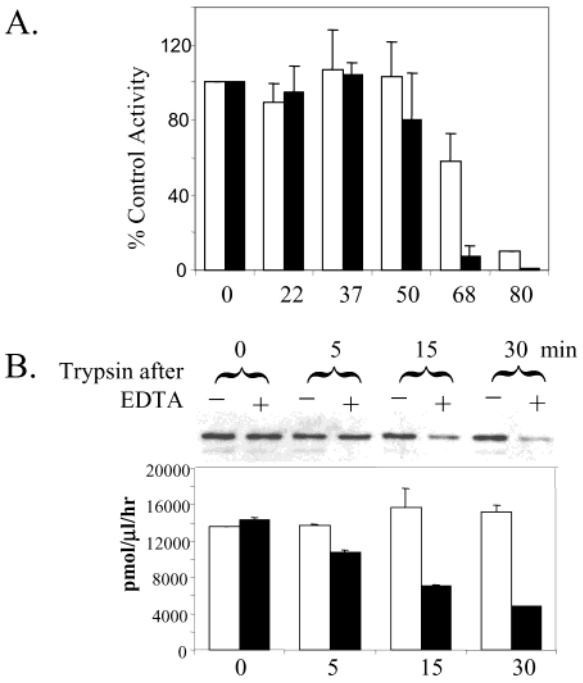

FIGURE 8: Structural role for metals in PALcc. (A) Aliquots of concentrated spent medium from stably transfected, nonclonal pEAK Rapid hEK-293 cells expressing PALcc were diluted 10-fold into 20 mM Tris-HCl (pH 8.0) and incubated at the indicated temperature for 30 min in the absence (empty bars) or presence (filled bars) of 4.0 mM EDTA. Samples were then chilled on ice, and aliquots were taken for SDS−PAGE (not shown) and for enzyme assays. (B) Spent medium (collected without protease inhibitors) diluted as described above was incubated at 37 °C for the indicated amount of time in the absence or presence of 1 mM EDTA; samples were then digested with trypsin for 30 min before Western blot analysis and measurement of enzyme activity were carried out.

includes exon 20, which encodes the first two Cys residues. Metabolic labeling studies indicate that half of the newly synthesized PHM/PAL674s has disappeared after 2 h of chase and secretion is not observed (Figure 7D). PHM/PAL741s includes all four Cys residues but still yields an inactive protein that fails to undergo secretion; unlike PHM/PAL674s, metabolic labeling studies indicate that PHM/PAL741s turns over slowly (Figure 7D). It is only upon inclusion of residues up to the second pair of basic amino acids encoded by exon 24 that active PAL is secreted (PAM-3/820s) (*9*).

Metals Play a Structural Role in PALcc. The earliest data on PAL suggested an essential role for divalent metals (*6*). More recent studies have identified both zinc and copper bound to soluble, bifunctional PAM (*29*). The copper is essential for PHM activity (*12*, *30*), and zinc may play a role in the lyase reaction (*29*). Since zinc can play both structural and catalytic roles in enzymes (*19*, *31*, *32*), we evaluated the effect of EDTA on the sensitivity of PALcc to thermal denaturation and to trypsin (Figure 8). PALcc was exposed to the indicated temperature for 30 min in the absence or presence of EDTA, chilled on ice, diluted, and subjected to an enzyme assay after addition of exogenous metal (Figure 8A). PALcc is remarkably resistant to thermal denaturation, retaining more than half of its activity after a 30 min incubation at 68 °C. In the presence of EDTA (filled bars), the enzyme is almost totally inactivated following a similar incubation.

We next asked whether prior exposure to EDTA affected the sensitivity of PALcc to trypsin (Figure 8B). Without preincubation with EDTA, PALcc incubated at 37 °C for up to 30 min was completely resistant to subsequent trypsin digestion; no smaller products were generated, and PAL activity was unaltered. Following exposure to EDTA, trypsin degraded most of the PALcc without generating a 33 kDa intermediate; the lack of the 33 kDa intermediate suggests that EDTA-treated PALcc has lost the structural constraints that normally give rise to this product. These data suggest that divalent metals play a major structural role in PALcc.

Identification of 1 mol of zinc/mol of bifunctional amidating enzyme led to the suggestion that PAL contains zinc (*18*). We used 4-(2-pyridylazo)resorcinol (PAR) to determine whether purified PALcc contained zinc (*23*). Native PALcc and PALcc denatured with guanidine HCl or with perchloric acid were examined (Table 1). Similar results were obtained with both methods. Separation by ion exchange resolves variable amounts of PALcc eluting around 175 and ~250

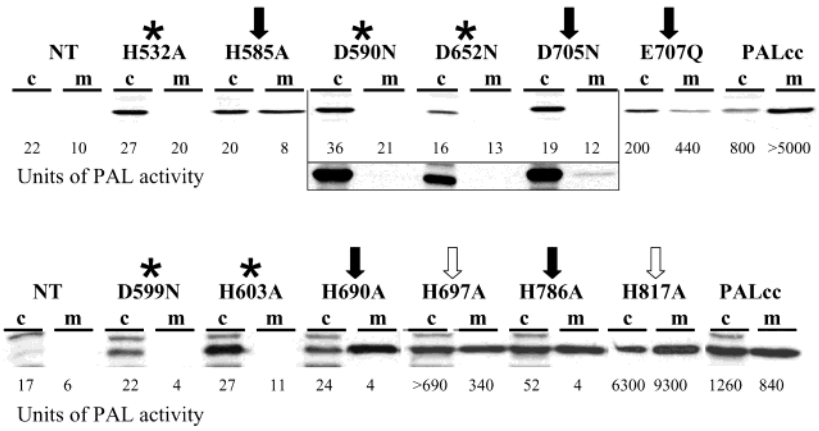

FIGURE 9: Site-directed mutagenesis of PALcc. His residues were mutated to Ala, Asp to Asn, and Glu to Gln (see Figure 1 for location). Production and secretion of each PALcc mutant were evaluated by Western blot analysis. The amount of activity associated with each sample is indicated (units of PAL activity, picomoles per hour); these assays used a concentration of substrate (0.5 μM) far below the K_m of the enzyme for its peptide substrate. Mutants were analyzed in three batches; nontransfected cells and cells expressing wild-type PALcc were analyzed simultaneously, but are only shown twice. The samples on the top row were analyzed simultaneously; a longer exposure is shown for three samples. On the bottom row, H817A was analyzed separately. Medium samples were collected over a 16 h period, and 1.6% of the medium sample was analyzed; 6.4% of the cell extract was analyzed. Independent transfections were analyzed and yielded similar results: (asterisk) nonsecreted, (filled arrow) secreted, and (empty arrow) nonconserved residue.

Table 1: Purified PALcc Contains Zinc[a]

sample	PALcc Q/R (μM)	[zinc] (μM)	zinc/PALcc (mol/mol)
MonoQ, pool A			
Prep-5-1	11.2	5.41	0.39
Prep-1-2	1.07	1.32	1.24
Prep-2-2	6.26	1.84	0.29
MonoQ, pool B			
Prep-1-2	1.36	0.94	0.69
Prep-2-2	8.47	7.92	0.94
Prep-3-13	1.69	0.88	0.52
		PALcc average	0.68 ± 0.36
bifunctional amidating enzyme (*18*)			1.1 ± 0.2

[a] PALcc elutes from the MonoQ column in two peaks, which were pooled and analyzed separately; pool A elutes at ~175 mM NaCl, and pool B elutes at ~250 mM NaCl. Several different preparations of purified PALcc were analyzed. The purified protein was denatured and analyzed for zinc using 4-(2-pyridylazo)resorcinol (PAR) (*23*). A standard curve was evaluated simultaneously.

mM NaCl. These pools of PALcc were analyzed separately. In general, material eluting earlier contained lower levels of zinc than material eluting later. On average, PALcc contained 0.68 ± 0.36 mol of zinc.

Site-Directed Mutagenesis of PALcc. Mutagenesis of PHM was initially guided by earlier studies of DBM, a homologous enzyme. Without a homologue, this approach is not available for PAL. Reasoning that zinc plays a unique role in PAL, we directed our attention to residues that might be involved in binding this metal ion. Since the Cys residues in PALcc are not available to bind zinc, conserved His, Asp, and Glu would be expected to play a major role (*19*, *20*, *31*, *33*) (Figure 1). The five conserved His residues were each mutated to Ala, while the four conserved Asp and single conserved Glu were mutated to Asn and Gln, respectively. Two nonconserved His residues were mutated to Ala as controls. Mutant PALcc proteins were transiently expressed in mammalian cells.

The effect of each mutation was first evaluated by comparing the amount of PALcc protein and enzyme activity recovered from cell extracts and media (Figure 9). Following transient transfection, the specific activity of PALcc in cell extracts was typically 40−200 pmol μg^{-1} h^{-1}, and the amount of PALcc protein secreted during a 16 h collection period equaled or exceeded the amount of PALcc protein found in 4-fold more cell extract (Figure 9). The ability of cells to secrete a mutant protein efficiently is taken as an indication that the protein has folded and acquired enough of the native structure to exit the endoplasmic reticulum.

The PALcc mutants were separated into a secretion competent group (group 1, downward arrows) and a secretion incompetent group (group 2, asterisk). As predicted, PALcc mutated at the nonconserved His residues (His^{697} and His^{817}) was secreted as well as PALcc and was active (empty arrows). Similarly, PALcc mutated at His^{585}, His^{690}, or His^{786} was secreted essentially as well as PALcc. In contrast, PALcc bearing mutations at Asp^{705} or Glu^{707} was secreted much less efficiently than PALcc; detection of PALcc-D705N in spent medium required a substantially increased exposure time (Figure 9, top panel). Although PAL mutated at Glu^{707} had a substantial amount of catalytic activity (Figure 9), it was clear that PALcc bearing a His^{585}, His^{690}, Asp^{705}, or His^{786} mutation was distinctly less active than wild-type PALcc.

No PAL protein was detected in the medium of cells expressing PALcc bearing a His^{532}, Asp^{590}, Asp^{599}, His^{603}, or Asp^{652} mutation (group 2). Consistent with this, no PAL activity could be attributed to these mutant PALcc proteins in cell extracts. Despite transfection with equal amounts of plasmid DNA, cells expressing PALcc bearing the Asp^{652} mutation consistently yielded lower levels of PAL expression. The possibility that this protein was unstable was explored in a pulse−chase metabolic labeling experiment; rapid intracellular degradation of PALcc bearing the Asp^{652} mutation was observed (data not shown).

Samples of medium were concentrated to assess more accurately the effect of each group 1 mutation on catalytic activity. Aliquots yielding known amounts of activity (assayed with a concentration of peptidyl-α-hydroxyglycine substrate 30-fold below the K_m) were evaluated for PAL protein content by Western blot (Figure 10A). A 30−60-fold drop in specific activity is observed for PALcc bearing

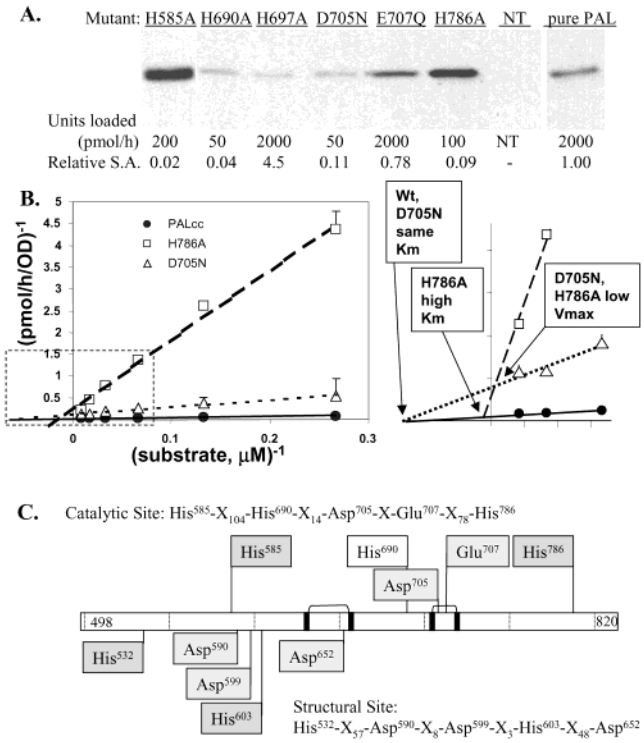

FIGURE 10: Specific activity of secreted PALcc mutants. (A) Concentrates of spent media were assayed for PAL activity using 0.5 μM α-*N*-acetyl-Tyr-Val-hydroxyglycine, a concentration far below the K_m; samples containing the indicated amount of activity were then fractionated by SDS−PAGE and visualized using antibody to a region of PAL that was not mutated. The amount of PAL protein was determined by Western blot analysis using an antipeptide antiserum to a region of PAL that was not mutated. Data from at least two independent transfections were quantified and averaged, and relative specific activities are indicated below each sample (picomoles of product per unit of PAL protein; the specific activity of PALcc was normalized to 1.0). (B) Relative V_{max} and K_m determinations for PALcc-H786A and PALcc-D705N. Concentrates were assayed with 1.8−60 μM α-*N*-acetyl-Tyr-Val-hydroxyglycine; the concentration of the PAL protein was determined by quantitative Western blot analysis. Data shown in Figure 3B were determined using the same preparation of α-*N*-acetyl-Tyr-Val-hydroxyglycine; a new preparation of the PAL substrate was used for the experiments reported here and in Table 2 and gave K_m values that were approximately 2-fold lower, presumably reflecting the greater purity of substrate prepared with more highly purified PHMcc. (C) Diagram summarizing the effects of the various mutations in PALcc. Mutations making up group 1 (secreted) are shown above the bar; mutations making up group 2 (not secreted) are shown below the bar.

the His^{585}, His^{690}, or His^{786} mutation; each of these mutant PALcc proteins is efficiently secreted. PALcc bearing the Asp^{705} mutation is secreted poorly and retains less than 5% of the wild-type activity. Mutation of Glu^{707} to Gln slowed secretion of PALcc, but the secreted protein was almost fully active. Mutations at any of three nonconserved sites (His^{697}, His^{817}, and Gln^{551}) yielded fully active, rapidly secreted protein (data not shown).

To screen for the effect of each mutation on K_m and V_{max}, kinetic parameters were determined for each group 1 PALcc mutant using Eadie−Hofstee (Table 2) and Lineweaver−Burk plots (Figure 10B). PALcc bearing the H786A mutation had a substantially increased K_m for α-*N*-acetyl-Tyr-Val-hydroxyglycine along with a decreased V_{max}, resulting in a 100-fold reduction in V_{max}/K_m, which is proportional to the specificity constant (Table 2). Mutation of His^{585} or His^{690} to Ala reduced V_{max} 50−100-fold with no detectable effect on K_m. In addition to a greatly diminished rate of secretion, PALcc bearing the D705N mutation had a decreased V_{max}, resulting in a more than 30-fold drop in its specificity constant. In contrast, mutation of Gln^{707} yielded an enzyme that was secreted slowly but was fully active.

Table 2: Kinetic Analysis of Group 2 Mutant PALcc[a]

	K_m (μM)	relative V_{max}	V_{max}/K_m
PALcc	13.9 ± 5.3	1.00 ± 0.23	1.00 ± 0.22
H585A	23.1 ± 6.0	0.016 ± 0.002[b]	0.0093 ± 0.0017[b]
H690A	15.6 ± 4.7	0.021 ± 0.016[b]	0.021 ± 0.020[b]
D705N	21.4 ± 19.0	0.079 ± 0.063[b]	0.089 ± 0.076[b]
E707Q	10.2 ± 5.0	0.48 ± 0.18	0.69 ± 0.31
H786A	98.5 ± 2.3[b]	0.07 ± 0.01[b]	0.0093 ± 0.0014

[a] Spent medium from transiently transfected pEAK Rapid cells expressing the indicated PALcc protein was concentrated, and the amount of PALcc protein in each sample was determined by quantitative Western blot analysis. The substrate concentration was varied from 1.8 to 120 μM, and kinetic parameters were determined using an Eadie−Hofstee plot. Data from at least two independent transfections were quantified and averaged; the specific activity of PALcc was normalized to 1.0. [b] Significantly different from that of PALcc ($p < 0.004$, *t* test, two-tailed, unequal variances).

These data suggest that His^{585}, His^{690}, Asp^{705}, and His^{786} are part of the PALcc catalytic site (Figure 10C). The fact that mutation of His^{786} has the greatest effect on the K_m of the enzyme for α-*N*-acetyl-Tyr-Val-hydroxyglycine suggests that residues near the COOH terminus of PALcc are involved in forming the substrate binding site. Mutants yielding a protein that cannot be secreted (His^{532}, Asp^{590}, Asp^{599}, His^{603}, and Asp^{652}) could individually play an essential role in enzyme structure or could jointly form a metal binding site.

DISCUSSION

PALcc Forms a Single Domain. PALcc extends from Asp^{498}, immediately following exon 16, to Val^{820}. A PAL protein with exactly this COOH terminus may be generated by prohormone convertase-mediated cleavage at the Lys^{821}−Lys bond followed by trimming by a carboxypeptidase B-like enzyme. The bifunctional α-amidating enzyme studied by Merkler et al. has this COOH terminus (*18*, *34*). Although the pro region of PAM was included in our expression vector to facilitate secretion (*35*), its presence is not essential for activity. The properties of PALcc are essentially identical to those of purified bovine PAL and to those of the lyase domain of recombinant PAM-3. Elimination of the single N-glycosylation site in PAL did not alter its kinetic parameters. The pH optimum of PAL is similar whether it is monofunctional or part of the bifunctional enzyme, as are K_m and V_{max} (*1*). Elimination of lyase activity following treatment with chelators and restoration following addition of a variety of divalent metal ions is observed for both monofunctional and bifunctional forms of PAL. In contrast, the properties of the monooxygenase domain are different when it functions as part of a bifunctional PAM protein instead of as a monofunctional enzyme.

PALcc, even lacking its N-linked oligosaccharide chain, is remarkably resistant to denaturants. A 50% reduction in PAL activity requires exposure to high levels of mercaptoethanol (125 mM), suggesting that both disulfide bonds are relatively inaccessible (*36*). Fully 50% of the catalytic activity remains after PALcc is incubated at 68 °C for 30 min. A

10-fold reduction in the activity of PAL requires the addition of approximately 10 mM EGTA or EDTA. Our data suggest that divalent metal ions play a role in stabilizing the structure of PAL because both the protease sensitivity and thermal sensitivity of PAL increase substantially upon pretreatment with EDTA.

PALcc does not fold into separable domains. As trypsin digestion proceeds beyond the inactive 33 kDa fragment, antibodies to PAL lose the ability to recognize any fragments. This result is consistent with our earlier studies on the protease sensitivity of PAM-3, where the smallest active PAL fragment that was generated had a mass of ~40 kDa (*17*). In contrast, endoproteinase LysC separated NH_2- and COOH-terminal domains of the catalytic core of PHM, rendering the enzyme inactive (*8*).

Analysis of the series of PHM/PALs proteins supports the conclusion that PALcc folds into a single domain. For this analysis, it is important to note that PAM-3 with a Lys-Asp-Glu-Leu endoplasmic reticulum retention/retrieval motif appended to its COOH terminus (PAM-3/KDEL) is retained in the endoplasmic reticulum and still yields fully active PHM and PAL when assayed in cell lysates (*37*). Thus, the environment in the lumen of the endoplasmic reticulum is compatible with proper folding and maturation of both catalytic domains. Appending the first three exons of PAL to PHM yields a protein that is readily secreted. As additional PAL exons are included, secretion is blocked, presumably reflecting binding of chaperone proteins to the malfolded, truncated lyase domain. A PHM/PAL protein is not secreted until the region between the Arg^{779}-Lys and Lys^{821}-Lys sequences is included. Consistent with this, one of the essential, conserved His residues, His^{786}, occurs in this region. Although the charged nature of the Arg^{779}-Lys sequence might predict a surface location, this potential tryptic cleavage site is inaccessible, indicating that it is buried in native PALcc.

PALcc Binds Zinc. A role for divalent metals in the lyase reaction was predicted on the basis of the effects of chelators, but a role for zinc was first proposed when purified bifunctional PAM was shown to contain zinc (*18*). The zinc stoichiometry determined from analysis of six samples from four different enzyme preparations was 0.68 ± 0.36 mol of Zn(II)/mol of PALcc (Table 1). The Zn(II) atom in PALcc and PAM must be tightly bound, since treatment of enzyme with either metal-free or Chelex-100-treated buffer gave identical Zn(II) stoichiometries. Zinc, the second most abundant trace metal in most higher animals, binds tightly to most zinc metalloproteins and serves catalytic and structural roles in a wide variety of proteins (*19*, *31*, *33*). A number of enzymes have both structural and catalytic metal binding sites (*19*). We used the presence of a zinc binding site to guide the site-directed mutagenesis of PALcc. The side chains of Cys, His, Asp, and Glu would be expected to play a role in binding zinc; since the four conserved Cys residues in PALcc are involved in disulfide bonds, we focused on His, Asp, and Glu.

Structural and Catalytic Effects of Mutagenesis. Mutagenesis of potential metal ion ligands yielded PALcc proteins that were secreted (group 1) and PALcc proteins that were not secreted (group 2). EXAFS studies indicate that the single zinc bound to the bifunctional amidating enzyme has two or three His and two non-His O/N ligands (*18*). On the basis of our analysis of monofunctional PAL, this zinc binding site is in PALcc. A site of the type identified by EXAFS could be formed by the side chains of group 1 (H^{585}, H^{690}, D^{705}, E^{707}, or H^{786}) or group 2 (H^{532}, D^{590}, D^{599}, H^{603}, or D^{652}). The most common ligand to catalytic zinc is His, followed by Glu, Asp, and Cys (*19*, *33*). Catalytic zinc ions are usually exposed and bound to a solvent molecule. Structural sites for zinc generally involve Cys, His, and occasionally Asp or Glu. At structural sites, zinc is buried and difficult to remove with chelators.

The side chains of the group 1 mutants (H^{585}, H^{690}, D^{705}, E^{707}, or H^{786}) provide insight into the catalytic site of PAL. PALcc mutated at E^{707}, although secreted poorly, is close to fully active. The fact that mutation of His^{786} to Ala increases the K_m of the enzyme for its peptidyl-α-hydroxyglycine substrate suggests a role for the COOH terminus of PAL in ligand binding and is consistent with the failure of PAM proteins truncated at Val^{778} to fold properly. Mutation of H^{585}, H^{690}, D^{705}, or H^{786} reduces V_{max}/K_m more than 30-fold. All three His residues in this group are preceded in the sequence by a Pro residue, perhaps providing added rigidity. If zinc plays a catalytic role, it could be bound at a site formed by these residues. The spacing of H^{585}, H^{690}, D^{705}, and H^{786} does not match that of any known catalytic zinc sites (*19*). Bound zinc could play a direct role in catalysis (*18*, *38*), or a zinc-coordinated water or hydroxide, acting as a general base, could abstract the hydroxyl proton of the carbinolamide. Alternatively, the side chains of His and Asp could participate directly in the acid−base catalysis of the reaction.

The group 2 PALcc mutants (H^{532}, D^{590}, D^{599}, H^{603}, or D^{652}) are inactive and are not secreted. Disruption of metal ion binding to a structural site would be expected to yield this phenotype. The single zinc bound to PALcc might be bound at a site formed by these residues. Consistent with the essential role determined for His^{532}, the 33 kDa product of trypsin digestion, which begins at Gly^{553}, lacks activity. The effect of EDTA pretreatment on the protease sensitivity and thermal stability of PALcc suggests a structural role for a divalent metal. Similarly, the inability to fully reconstitute catalytic activity following prolonged EDTA-mediated removal of zinc from the bifunctional amidating enzyme led to the proposal that zinc plays a structural role (*18*). Mutagenesis of potential metal ion ligands yielded results for PAL very different from those observed previously for PHM. Although each of the five conserved His residues in PHM proved to be an essential copper ligand, mutation yielded inactive proteins that were secreted efficiently (*26*, *30*). In PHM, copper ligands were essential for catalytic activity, but not for structure. The structure of PAL proved to be much more sensitive to mutation.

Homologues of PALcc. Ureidoglycolate lyase (EC 4.3.2.3), which produces urea and glyoxalate, catalyzes a reaction very similar to that catalyzed by PAL. Ureidoglycolate lyase was purified from rat liver mitochondria and from fish liver peroxisomes (*39*, *40*) and from chickpea pods (*41*). Both the fish liver enzyme and the chickpea enzyme are activated by bivalent metal ions (*39*, *41*). Sequence data are not available for any of these ureidoglycolate lyases.

A BLASTP search of the nonredundant GenBank CDS Database identified segments of PAL that are homologous to *Caenorhabditis elegans* LIN-41A and B, *Mycobacterium tuberculosis* serine/threonine protein kinase (X99618.2), and

human HT2A (AL133284.13), a zinc-finger protein. The regions of homology fall within NHL repeats (*42*). NHL repeats, first recognized in NCL-1, HT2A, and LIN-41, contain almost invariant Pro and Asp residues and are rich in Gly and hydrophobic residues. The NHL domain of PAL is composed of four NHL repeats. H^{585}, H^{690}, and H^{786}, three of the residues postulated to form a catalytic site, occur immediately after the Pro residue that defines the start of an NHL repeat. Three of the essential Asp residues (D^{599}, D^{652}, and D^{705}) correspond to the almost invariant Asp defining the C-terminus of NHL repeats. Except for H^{532}, all of the residues identified as being essential occur within one of the four NHL repeats. The yeast genome does not encode proteins that are homologous to PAL, and NHL domains have not been identified in *Saccharomyces cerevisiae* or in *Escherichia coli* (*42*).

Crystallographic studies and further structural studies will reveal the nature of the active site and any structural relationship of PAL to known enzymes. In particular, it will be clear whether the residues identified in our mutagenesis studies actually form a binding site for zinc. The reason mutation of so many conserved Asp, Glu, and His residues disrupts the structure of PALcc should also become apparent.

ACKNOWLEDGMENT

We gratefully acknowledge the help of Marie Bell and Darlene D'Amato, without whom this work could not have been completed. We also thank Drs. Sharon Milgram and Fred Nucifore, who initiated our studies on truncated PAM proteins.

REFERENCES

1. Eipper, B. A., Perkins, S. N., Husten, E. J., Johnson, R. C., Keutmann, H. T., and Mains, R. E. (1991) *J. Biol. Chem. 266*, 7827−7833.
2. Merkler, D. J. (1994) *Enzyme Microb. Technol. 16*, 450−456.
3. Ping, D., Katopodis, A. G., and May, S. W. (1992) *J. Am. Chem. Soc. 114*, 3998−4000.
4. Ping, D., Mounier, C. E., and May, S. W. (1995) *J. Biol. Chem. 270*, 29250−29255.
5. Takahashi, K., Okamoto, H., Seino, H., and Noguchi, M. (1990) *Biochem. Biophys. Res. Commun. 169*, 524−530.
6. Perkins, S. N., Husten, E. J., and Eipper, B. A. (1990) *Biochem. Biophys. Res. Commun. 171*, 926−932.
7. Grimmelikhuijzen, C. J. P., Darmer, D., Schmutzler, C., Reinscheid, R. K., and Carstensen, K. (1994) *Perspect. Comp. Endocrinol.*, 97−108.
8. Kolhekar, A. S., Keutmann, H. T., Mains, R. E., Quon, A. S. W., and Eipper, B. A. (1997) *Biochemistry 36*, 10901−10909.
9. Kolhekar, A. S., Quon, A. S. W., Berard, C. A., Mains, R. E., and Eipper, B. A. (1998) *J. Biol. Chem. 273*, 23012−23018.
10. Kolhekar, A. S., Roberts, M. S., Jiang, N., Johnson, R. C., Mains, R. E., Eipper, B. A., and Taghert, P. H. (1997) *J. Neurosci. 17*, 1363−1376.
11. Klinman, J. P., and Huyghe, B. G. (1991) *J. Biol. Chem. 266*, 11544−11550.
12. Blackburn, N. J., Rhames, F. C., Ralle, M., and Jaron, S. (1999) *J. Biol. Inorg. Chem. 5*, 341−353.
13. DeWolf, W. E., Jr., Chambers, P. A., Southan, C., Saunders, D., and Kruse, L. I. (1989) *Biochemistry 28*, 3833−3842.
14. Kulathila, R., Merkler, K. A., and Merkler, D. J. (1999) *Nat. Prod. Rep. 16*, 145−154.
15. Katopodis, A. G., Ping, D., Smith, C. E., and May, S. W. (1991) *Biochemistry 30*, 6189−6194.
16. Husten, E. J., and Eipper, B. A. (1991) *J. Biol. Chem. 266*, 17004−17010.
17. Husten, E. J., Tausk, F. A., Keutmann, H. T., and Eipper, B. A. (1993) *J. Biol. Chem. 268*, 9709−9717.
18. Bell, J., Ash, D. E., Snyder, L. M., Kulathila, R., Blackburn, N. J., and Merkler, D. J. (1997) *Biochemistry 36*, 16239−16246.
19. Alberts, I. L., Nadassy, K., and Wodak, S. J. (1998) *Protein Sci. 7*, 1799−1716.
20. Christianson, D. W., and Cox, J. D. (1999) *Annu. Rev. Biochem. 68*, 33−57.
21. Aitken, A., and Learmonth, M. (1996) in *The Protein Protocols Handbook* (Walker, J. M., Ed.) pp 487−488, Humana Press, Inc., Totawa, NJ.
22. Fontana, A. (1972) *Methods Enzymol. 25*, 419.
23. Hunt, J. B., Neece, S. H., and Ginsburg, A. (1985) *Anal. Biochem. 146*, 150−157.
24. Milgram, S. L., Johnson, R. C., and Mains, R. E. (1992) *J. Cell Biol. 117*, 717−728.
25. Milgram, S. L., Eipper, B. A., and Mains, R. E. (1994) *J. Cell Biol. 124*, 33−41.
26. Eipper, B. A., Quon, A. S. W., Mains, R. E., Boswell, J. S., and Blackburn, N. J. (1995) *Biochemistry 34*, 2857−2865.
27. Aslund, F., and Beckwith, J. (1999) *Cell 96*, 751−753.
28. Bloomquist, B. T., Eipper, B. A., and Mains, R. E. (1991) *Mol. Endocrinol. 5*, 2014−2024.
29. Ash, D. E., Papadopoulos, N. J., Colombo, G., and Villafranca, J. J. (1984) *J. Biol. Chem. 259*, 3395−3398.
30. Prigge, S. T., Kolhekar, A. S., Eipper, B. A., Mains, R. E., and Amzel, L. M. (1997) *Science 278*, 1300−1305.
31. Berg, J. M., and Godwin, H. A. (1997) *Annu. Rev. Biophys. Biomol. Struct. 26*, 357−371.
32. Coleman, J. E. (1992) *Annu. Rev. Biochem. 61*, 897−946.
33. Berg, J. M., and Shi, Y. (1996) *Science 271*, 1081−1085.
34. Miller, D. A., Sayad, K. U., Kulathila, R., Beaudry, G. A., Merkler, D. J., and Bertelsen, A. H. (1992) *Arch. Biochem. Biophys. 298*, 380−388.
35. Mains, R. E., Milgram, S. L., Keutmann, H. T., and Eipper, B. A. (1995) *Mol. Endocrinol. 9*, 3−13.
36. Huppa, J. B., and Ploegh, H. L. (1998) *Cell 92*, 145−148.
37. Yun, H.-Y., and Eipper, B. A. (1995) *J. Biol. Chem. 270*, 15412−15416.
38. Prigge, S. T., Mains, R. E., Eipper, B. A., and Amzel, L. M. (2000) *Cell. Mol. Life Sci. 57*, 1236−1259.
39. Takada, Y., and Noguchi, T. (1986) *Biochem. J. 235*, 391−397.
40. Fujiwara, S., and Noguchi, T. (1995) *Biochem. J. 312*, 315−318.
41. Munoz, A., Piedras, P., Aguilar, M., and Pineda, M. (2001) *Plant Physiol. 125*, 828−834.
42. Slack, F. J., and Ruvkun, G. (1998) *Trends Biochem. Sci. 23*, 474−475.
43. Stoffers, D. A., Green, C. B., and Eipper, B. A. (1989) *Proc. Natl. Acad. Sci. U.S.A. 86*, 735−739.

BI0260280